AZD6244 (ARRY-142886), a potent inhibitor of mitogen-activated protein kinase/extracellular signal-regulated kinase kinase 1/2 kinases: mechanism of action *in vivo*, pharmacokinetic/pharmacodynamic relationship, and potential for combination in preclinical models

Barry R. Davies,[1] Armelle Logie,[1] Jennifer S. McKay,[2] Paul Martin,[3] Samantha Steele,[2] Richard Jenkins,[2] Mark Cockerill,[1] Sue Cartlidge,[1] and Paul D. Smith[1]

[1]Cancer and Infection Research Area, [2]Global Safety Assessment, and [3]Drug Metabolism and Pharmacokinetics, AstraZeneca, Alderley Park, Macclesfield, United Kingdom

Abstract

Constitutive activation of the extracellular signal-regulated kinase 1/2 (ERK1/2) mitogen-activated protein kinase (MAPK) signaling pathway in human cancers is often associated with mutational activation of BRAF or RAS. MAPK/ERK kinase 1/2 kinases lie downstream of RAS and BRAF and are the only acknowledged activators of ERK1/2, making them attractive targets for therapeutic intervention. AZD6244 (ARRY-142886) is a potent, selective, and ATP-uncompetitive inhibitor of MAPK/ERK kinase 1/2. *In vitro* cell viability inhibition screening of a tumor cell line panel found that lines harboring *BRAF* or *RAS* mutations were more likely to be sensitive to AZD6244. The *in vivo* mechanisms by which AZD6244 inhibits tumor growth were investigated. Chronic dosing with 25 mg/kg AZD6244 bd resulted in suppression of growth of Colo-205, Calu-6, and SW-620 xenografts, whereas an acute dose resulted in significant inhibition of ERK1/2 phosphorylation. Increased cleaved caspase-3, a marker of apoptosis, was detected in Colo-205 and Calu-6 but not in SW-620 tumors where a significant decrease in cell proliferation was detected. Chronic dosing of AZD6244 induced a morphologic change in SW-620 tumors to a more differentiated phenotype. The potential of AZD6244 in combination with cytotoxic drugs was evaluated in mice bearing SW-620 xenografts. Treatment with tolerated doses of AZD6244 and either irinotecan or docetaxel resulted in significantly enhanced antitumor efficacy relative to that of either agent alone. These results indicate that AZD6244 has potential to inhibit proliferation and induce apoptosis and differentiation, but the response varies between different xenografts. Moreover, enhanced antitumor efficacy can be obtained by combining AZD6244 with the cytotoxic drugs irinotecan or docetaxel. [Mol Cancer Ther 2007;6(8):2209–19]

Introduction

The signaling pathway comprising mitogen-activated protein kinase (MAPK)/extracellular signal-regulated kinase (ERK) kinase (MEK) and ERK is activated in most human tumors. Signaling through this pathway occurs following activation of cell surface receptors by extracellular ligands, constitutive activation of cell surface receptors by mutation or overexpression, or more commonly through gain-of-function mutations of BRAF and RAS family members. Activating mutations in RAS and BRAF typically show mutual exclusivity in tumors, suggesting that the proteins encoded by these genes deregulate a common effector pathway. The four ras GTPase proteins found in mammals (N-ras, H-ras, Kras4A, and K-ras4B) signal via at least three major effector cascades, including the raf kinases, type 1 phosphatidylinositol 3-kinases, and Ral guanine nucleotide exchange factors; these pathways operate differentially in discrete cell types. Mutations in K-ras occur in ~90% of pancreatic and in 25% to 50% of colorectal, mucinous ovarian, and non–small cell lung cancers, whereas mutations in H-ras are common in bladder, kidney, and thyroid cancers and N-ras mutations are found in melanoma, hepatocellular carcinoma, and hematologic malignancies (1–3). The three raf isoforms (Raf1, A-Raf, and B-raf) activate both MEK1 and MEK2. B-raf–activating mutations have been reported in ~60% of melanomas (4, 5), 70% of nonpapillary thyroid cancers (6, 7), ~35% of low-grade ovarian serous tumors (2, 8), 5% to 10% of colorectal cancers (4, 9), and <5% of non–small cell lung cancers (10).

MEK1/2 kinases show a unique specificity to ERK1/2, phosphorylating them on their activatory tyrosine and threonine residues. ERKs have a wide substrate specificity; >100 targets involved in a multitude of cellular responses have been reported. These include transcription factors, kinases and phosphatases, cytoskeletal proteins, and

Received 4/2/07; revised 5/31/07; accepted 7/2/07.

The costs of publication of this article were defrayed in part by the payment of page charges. This article must therefore be hereby marked *advertisement* in accordance with 18 U.S.C. Section 1734 solely to indicate this fact.

Note: A. Logie and J.S. McKay contributed equally to this work.

Requests for reprints: Barry R. Davies, Cancer and Infection Research Area, AstraZeneca, Mereside, Alderley Park, Macclesfield, Cheshire SK10 4TG, United Kingdom. Phone: 44-1625-514604; Fax: 44-1625-513624. E-mail: Barry.Davies@astrazeneca.com

doi:10.1158/1535-7163.MCT-07-0231

modulators of apoptosis (11). Many of the substrates of ERKs play a role in promoting cell proliferation and survival. Given that self-sufficiency of growth signals and evasion of cell death are key features of malignant neoplasms (12), and the dual specificity of MEK1/2 for ERK1/2, it follows that MEK1/2 kinases are attractive targets for cancer therapy.

AZD6244 (ARRY-142886) is a potent, selective, and ATP-uncompetitive inhibitor of MEK1/2 kinases and is currently in phase II clinical development (13, 14). In this report, the relationship between the pharmacodynamic inhibition of the primary biomarker [phosphorylated ERK (p-ERK)] and the plasma-free levels of the drug is described in Calu-6 xenografts growing in nude mice. We also report on the mechanism of action of this drug in sensitive xenografts, and the potential of this drug as a combinatorial agent, by describing the response of a colorectal xenograft to treatment with combinations of AZD6244 and cytotoxic agents.

Materials and Methods

Cell Culture

Colo-205 and SW-620 cells were obtained from the European Collection of Cell Cultures, and Calu-6 cells were obtained from the American Type Culture Collection. Cells were plated on T75 tissue culture flasks, routinely grown as monolayer cultures, and maintained in culture in L-15 (SW-620), RPMI 1640 (Colo-205), or Eagle's MEM (Calu-6) supplemented with 10% fetal bovine serum, 1% L-glutamine, 1% nonessential amino acid (Invitrogen), and 1% sodium pyruvate (Invitrogen) in a humidified environment of 5% CO_2/95% air at 37°C.

Animals

Specific, pathogen-free, female nude mice (*nu/nu:Alpk*) were bred in house. The mice were housed and maintained in specific, pathogen-free conditions. The facilities have been approved by the Home Office License and meet all current regulations and standards of the United Kingdom. The mice were used between the ages of 8 and 12 weeks in accordance with institutional guidelines.

Implantation of Cells into Mice

For *in vivo* implant, cells were harvested from T225 tissue culture flasks by a 2- to 5-min treatment with 3× trypsin (Invitrogen) in EDTA solution followed by suspension in basic medium and three washes in PBS (Invitrogen). Only single-cell suspensions of >90% viability, as determined by trypan blue exclusion, were used for injection. Tumor cells (1×10^6 for Calu-6 and SW-620; 2×10^6 for Colo-205) were injected s.c. in the left flank of the animal in a volume of 0.1 mL.

Efficacy Studies

When mean tumor size reached 0.2 cm^3, the mice were randomized into control and treatment groups. The treatment groups received 0.5, 2.5, 10, or 25 mg/kg twice daily of AZD6244 solubilized in a methocel/polysorbate buffer, by oral gavage, docetaxel (Aventis) at 15 mg/kg, solubilized in 2.6% ethanol in injectable water, or irinotecan (Aventis) at 25 mg/kg, solubilized in 5% glucose, once weekly by i.v. injection. When given in combination, the cytotoxic would be given 2 h after the oral dose. The control group received the methocel/polysorbate buffer alone, twice daily by oral gavage. Tumor volumes (measured by caliper), animal body weight, and tumor condition were recorded twice weekly for the duration of the study. Mice were sacrificed by CO_2 euthanasia. The tumor volume was calculated, taking length to be the longest diameter across the tumor and width to be the corresponding perpendicular diameter using the following formula: (length × width) × $\sqrt{}$(length × width) × (π / 6). Growth inhibition from the start of treatment was assessed by comparison of the differences in tumor volume between control and treated groups. Because the variance in mean tumor volume data increases proportionally with volume (and is therefore disproportionate between groups), data were log transformed to remove any size dependency before statistical evaluation. Statistical significance was evaluated using a one-tailed, two-sample t test. To analyze the data from the combination study, the statistical tool SigmaStat has been used. A two-way ANOVA test was done using the factors concentration of drug A and concentration of drug B. The data analyzed was log (final tumor volume) − log (initial tumor volume) calculated for each individual group at the end of the study. This tool is used to assess whether there is a main effect of drug A, a main effect of drug B, plus a significant interaction between the two compounds A and B (e.g., one compound influences the effect of the other compound), which may be interpreted as antagonism, additivity, or synergism.

Pharmacodynamic Studies

When mean tumor size reached 0.5 cm^3, the mice were randomized into control and treatment groups (n = 5 animals per group). The treatment groups received 25 mg/kg acute dose of AZD6244 solubilized in a methocel/polysorbate buffer, by oral gavage. The control group received the methocel/polysorbate buffer alone, once by oral gavage. The animals in the 4-, 8-, and 24-h groups received a single injection of bromodeoxyuridine (BrdUrd; Sigma) at 100 mg/kg i.p. 4 h before termination. At 2, 4, 8, 16, or 24 h after dose, the animals were humanely killed and the samples were collected. Half the tumor was snap frozen in liquid nitrogen and immediately frozen at −80°C for pharmacodynamic analysis; the other half was fixed in 10% formalin buffer for 24 h and then embedded in paraffin for immunohistochemical staining. Total blood was collected by intracardiac puncture, and plasma was prepared and immediately frozen at −20°C for pharmacokinetic analysis.

Plasma Pharmacokinetic Analysis

Plasma samples were extracted by protein precipitation in acetonitrile. Following centrifugation, the supernatants were evaporated to dryness under nitrogen and redissolved in high-performance liquid chromatography mobile phase. Extracts were analyzed by high-performance liquid chromatography/mass spectrometry using a reversed-phase Synergi Hydro-RP column (Phenomenex)

and a gradient mobile phase containing water/acetonitrile/formic acid. Peaks were detected using a Micromass ZQ2000 mass spectrometer. The assay had a range of 0.02 to 17 μg/mL.

Western Blotting and Cell Viability Studies

Frozen tumors were homogenized in liquid nitrogen using a freezer/mill (SPEX CertiPrep), and lysates were generated using adjusted radioimmunoprecipitation assay buffer. Equivalent amounts of protein (13.5 μg/lane) were resolved by 4% to 15% gradient SDS-polyacrylamide premade gels (Bio-Rad), transferred to nylon membranes, and incubated with anti–phosphorylated MAPK p44/p42 or anti-MAPK p44/p42 and subsequently with horseradish peroxidase–conjugated anti-rabbit IgG (Cell Signaling Technology). Immunoreactive proteins were detected by enhanced chemiluminescence (Pierce), and bands were quantified with a Chemigenious (Syngene).

In vitro cell viability was determined by the colorimetric 3-(4,5-dimethylthiazol-2-yl)-5-(3-carboxymethoxyphenyl)-2-(4-sulfophenyl)-2H-tetrazolium assay. In brief, cells were plated in 100 μL in 96-well plates at a density that generated continual linear growth. The cells were allowed to adhere overnight before exposure to AZD6244 for 72 h at 37°C. Plates were read using a spectrophotometer at a wavelength of 490 nm. All assays were carried out in triplicate at least twice.

Immunocytochemistry

Sections were dewaxed, and endogenous peroxidase activity was blocked with 3% (v/v) hydrogen peroxide for 10 min. All sections were heated in a Milestone Rapid Microwave Histoprocessor (model RHS-2) to retrieve antigen. Sections to be stained with anti-BrdUrd antiserum were placed in 0.001 mol/L EDTA buffer (pH 8) and incubated at 110°C for 2 min, whereas sections to be stained with cleaved caspase-3 and phosphorylated p44/42 MAPK were placed in 0.01 mol/L citrate (pH 6) and incubated for 2 min at 115°C and 110°C, respectively. Sections were cooled and those that were subsequently stained with anti-BrdUrd were treated with 2 mol/L hydrochloric acid for 30 min. Sections were then transferred to a Lab Vision Autostainer. Following incubation with 5% normal goat serum (Dako) for 20 min, sections were incubated with primary antibody at room temperature for 60 min (anti-BrdUrd, clone Bu20a, Dako; anti-cleaved caspase-3, Cell Signaling Technology; anti–phosphorylated p44/42 MAPK, Cell Signaling Technology). Alkaline phosphatase treatment (New England Biolabs) confirmed antibody specificity for the phosphorylated, and not the nonphosphorylated, form of anti–phosphorylated p44/42 MAPK in human xenografts. Additionally, the specificity of this antibody was also verified by Western blotting. Sections were subsequently incubated with mouse-labeled polymer from Mouse EnVision kit (Dako) or rabbit-labeled polymer from Rabbit EnVision kit (Dako) for 30 min at room temperature, and signal was detected using the EnVision kit 3,3′-diaminobenzidine (Dako). Sections were counterstained with Carazzi's hematoxylin and mounted with Histomount (Fisher Scientific).

Stained sections were analyzed using the Clarient ChromaVision Automated Cellular Imaging System. The Automated Cellular Imaging System is a color space image analyzer for which thresholds of hue, luminosity, and saturation were set relative to the chromogens used for the immunolocalization of cleaved caspase-3, BrdUrd, and p-ERK. The viable area of the whole section was selected and scored. The data generated an intensity value (the mean brown intensity of all the brown pixels), a brown area value (the cumulative area in μm^2 of all the brown pixels), and a blue area value (the cumulative area in μm^2 of all the blue pixels). The brown area value represents positive immunostaining, whereas the brown plus blue area values represent tissue area. The data analysis for cleaved caspase-3, BrdUrd, and p-ERK localization used a percentage labeling value as a measure of amount of target expressed in the xenograft. This labeling value was derived from the positive immunostaining value divided by tissue area value times 100. For each immunohistochemical method, a mean value and SE were calculated for each group and values were plotted using Microsoft Excel. An ANOVA, with appropriate contrasts, was used to compare data for each time point with the control data.

Results

Effect of AZD6244 on Viability of Human Tumor Cell Lines *In vitro*

Before evaluating the effect of AZD6244 treatment on xenografts in nude mice, the sensitivity of a large panel of cell lines to AZD6244 was evaluated *in vitro* and correlated with *RAS* and *BRAF* gene mutation status. There was a wide range of sensitivity to AZD6244 from highly sensitive (IC_{50}, <100 nmol/L) to highly resistant (>10 μmol/L; Fig. 1). In considering the effect of mutational activation of BRAF or RAS family proteins on the sensitivity to AZD6244, there is a clear, although not absolute, tendency for cell lines with *BRAF* and *RAS* gene mutations to be more sensitive to AZD6244 than those with wild-type genes. The cell lines selected for *in vivo* studies were Colo-205 (colorectal, mutant BRAF, 0.03 μmol/L), SW-620 (colorectal, mutant KRAS, 0.2 μmol/L), and Calu-6 (non–small cell lung cancer, mutant KRAS, 0.7 μmol/L).

Efficacy of AZD6244 in Human Tumor Xenografts in Nude Mice

When dosing was commenced at a mean tumor size of 0.2 cm^3, chronic dosing with 25 mg/kg bd AZD6244 completely inhibited growth of Colo-205 tumors (101% inhibition; $P < 0.0001$). A dose response was clearly observed in this model; 2.5 mg/kg bd partially inhibited growth and 0.5 mg/kg bd did not significantly inhibit growth (Fig. 2A). If dosing was commenced when the tumors reached a size of 0.5 cm^3, 25 mg/kg bd induced regression in this model (Fig. 2B). Calu-6 xenografts were also strongly growth inhibited by 25 and 10 mg/kg bd (94% and 88% inhibition, respectively; $P < 0.0001$; Fig. 2C). A dose response was also observed in this model at lower doses, with 0.75 mg/kg the minimum twice-daily dose

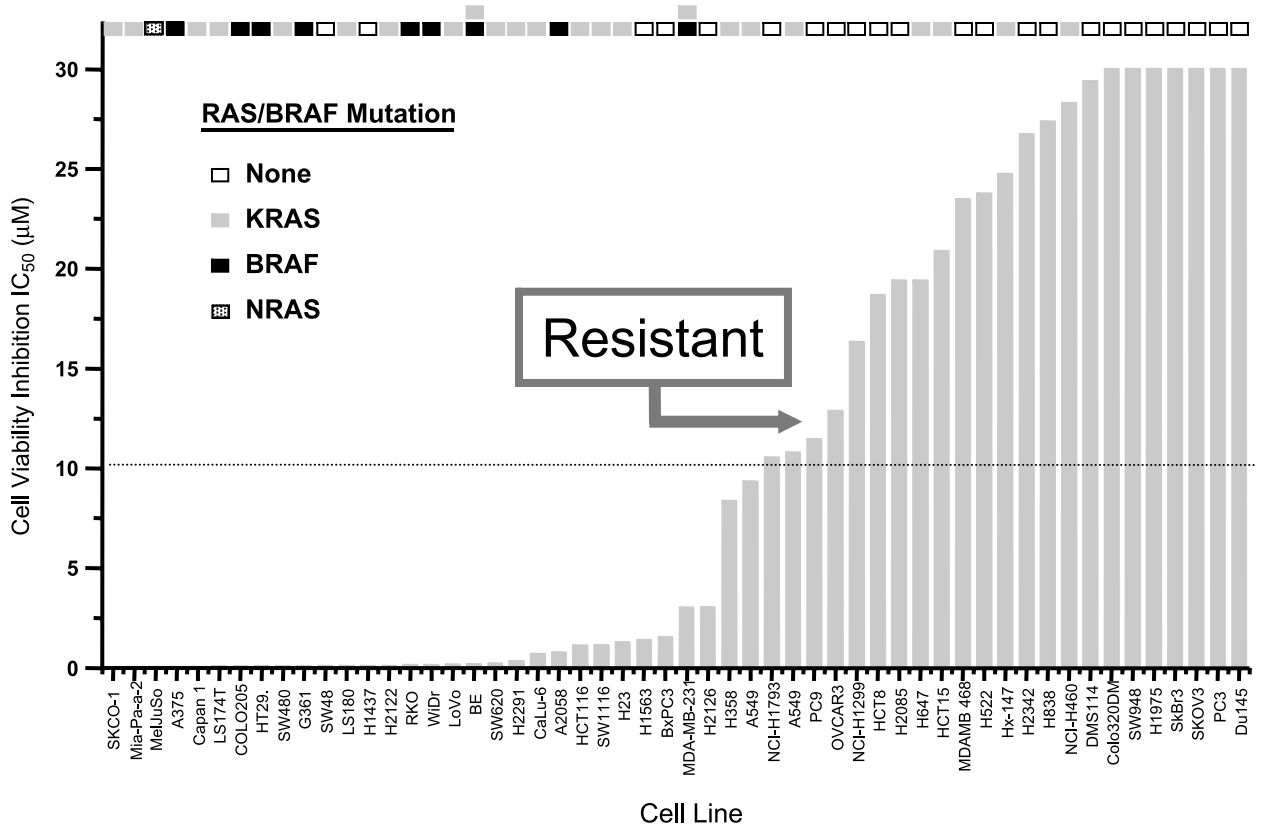

Figure 1. Viability of a panel of cell lines exposed to AZD6244. *In vitro* cell viability was determined by the colorimetric 3-(4,5-dimethylthiazol-2-yl)-5-(3-carboxymethoxyphenyl)-2-(4-sulfophenyl)-2H-tetrazolium assay.

that resulted in significant growth inhibition compared with vehicle alone (35% inhibition; $P = 0.009$; data not shown). Chronic dosing with 25 mg/kg bd AZD6244 caused partial growth inhibition of SW-620 xenografts (73% inhibition; $P < 0.0001$; Fig. 2D). The effect of once-daily versus twice-daily dosing of AZD6244 was compared in the Calu-6 model. The efficacy of 50 mg/kg qd was similar to 25 mg/kg bd (Supplementary Fig. S1).[4]

Pharmacodynamic Effects of AZD6244 in Calu-6 Xenografts

The effect of acute doses of 25 or 0.75 mg/kg AZD6244 on the level of the primary biomarker p-ERK was evaluated by immunohistochemistry and Western blotting of *ex vivo* tissue. In untreated control xenografts, the nucleus and cytoplasm stain strongly with antiserum to p-ERK. The perinuclear region stains particularly intensely in mitotic cells. After dosing with 25 mg/kg AZD6244, immunostaining in the cytoplasm and nucleus is reduced (Fig. 3A). Following an acute dose of 25 mg/kg, immunostaining in the cytoplasm was reduced by ~90% at 1, 2, and 4 h and recovered to >50% of the level of the control by 24 h. Staining of the nucleus followed a similar pattern (Fig. 3B). An acute dose of 0.75 mg/kg AZD6244, the lowest dose that gave significant antitumor activity, resulted in a similar trend, except the cytoplasmic staining was only reduced by ~80% at 1, 2, and 4 h, and the signal recovered more rapidly, exceeding 50% of control after 8 h (Fig. 3C). When lysates from the same tumors were analyzed for p-ERK expression by Western blotting, a similar trend was observed, although the Western blotting consistently gave a slightly higher signal than the immunohistochemistry (Fig. 3B and C).

Inhibition of p-ERK showed an inverse correlation with plasma drug concentration. The maximum free drug concentrations measured following doses of 25 and 0.75 mg/kg were ~160 and 16 ng/mL, respectively (350 and 35 nmol/L); these values are ~80- and 8-fold greater than the IC_{50} for inhibition of ERK phosphorylation in Calu-6 cells *in vitro* (Supplementary Fig. S2).[4] An acute dose of 25 mg/kg AZD6244 gives ~10 times greater exposure than 0.75 mg/kg (area under the plasma concentration versus time curves = 35.1 and 3.9 μg h/mL, respectively), indicating that there is a nonlinear relationship between dose and exposure to drug in between these doses in this nude mouse model. The concentration of free drug that results in ~50% inhibition of p-ERK in the cytoplasm *in vivo* shows a reasonable correlation with the *in vitro* IC_{50} for inhibition of ERK phosphorylation in cultured

[4] Supplementary material for this article is available at Molecular Cancer Therapeutics Online (http://mct.aacrjournals.org/).

cells of ~4.4 nmol/L (2 ng/mL; Fig. 3D; Supplementary Fig. S2).[4] Following doses of 25 and 0.75 mg/kg, levels of exposure greater than the *in vitro* IC_{50} were maintained up to 24 and 8 h, respectively.

Biomarkers of apoptosis (cleaved caspase-3) and proliferation (BrdUrd) were analyzed at various time points after an acute dose of 25 mg/kg bd AZD6244 in this model. Cleaved caspase-3 was significantly induced after 8 h and attained a magnitude of 3.3-fold greater than control at 16 h after dosing (Fig. 4A and B). Significant induction of cleaved caspase-3 was verified in snap-frozen *ex vivo* tissue from the same experiment by ELISA (data not shown). BrdUrd incorporation did not differ significantly from controls after 4 and 8 h but was significantly reduced at 24 h (Fig. 4B).

Pharmacodynamic Effects of AZD6244 in Colo-205 Xenografts

AZD6244 induced apoptosis in Colo-205 xenografts; the greatest mean induction of cleaved caspase-3 activity observed was ~6-fold at 8 h after dosing. A significant reduction in BrdUrd incorporation was detected 24 h after dosing (Fig. 4B).

An acute dose of 25 mg/kg AZD6244 resulted in a reduction in cytoplasmic and nuclear p-ERK in Colo-205 xenografts. However, the percentage reduction in p-ERK staining was not as great as that observed in Calu-6 xenografts; the maximum reduction of p-ERK was ~20% and ~50% of control in the nucleus and cytoplasm, respectively, 4 h after dosing with compound. The cytoplasmic signal recovered to a level that did not differ significantly from the controls after 24 h. The magnitude of reduction of the nuclear signal in this xenograft was consistently greater than the cytoplasmic signal, and the pharmacodynamic effect on p-ERK activity peaked later than plasma concentrations of drug (Fig. 4C).

Pharmacodynamic Effects of AZD6244 in SW-620 Xenografts

After an acute dose of 25 mg/kg AZD6244, p-ERK was maximally reduced after 8 h to ~26% and ~10% of the controls in the cytoplasm and nucleus, respectively. The time of maximum inhibition of p-ERK activity in this xenograft lagged considerably behind the peak plasma concentration of drug, and with the exception of the 16 h

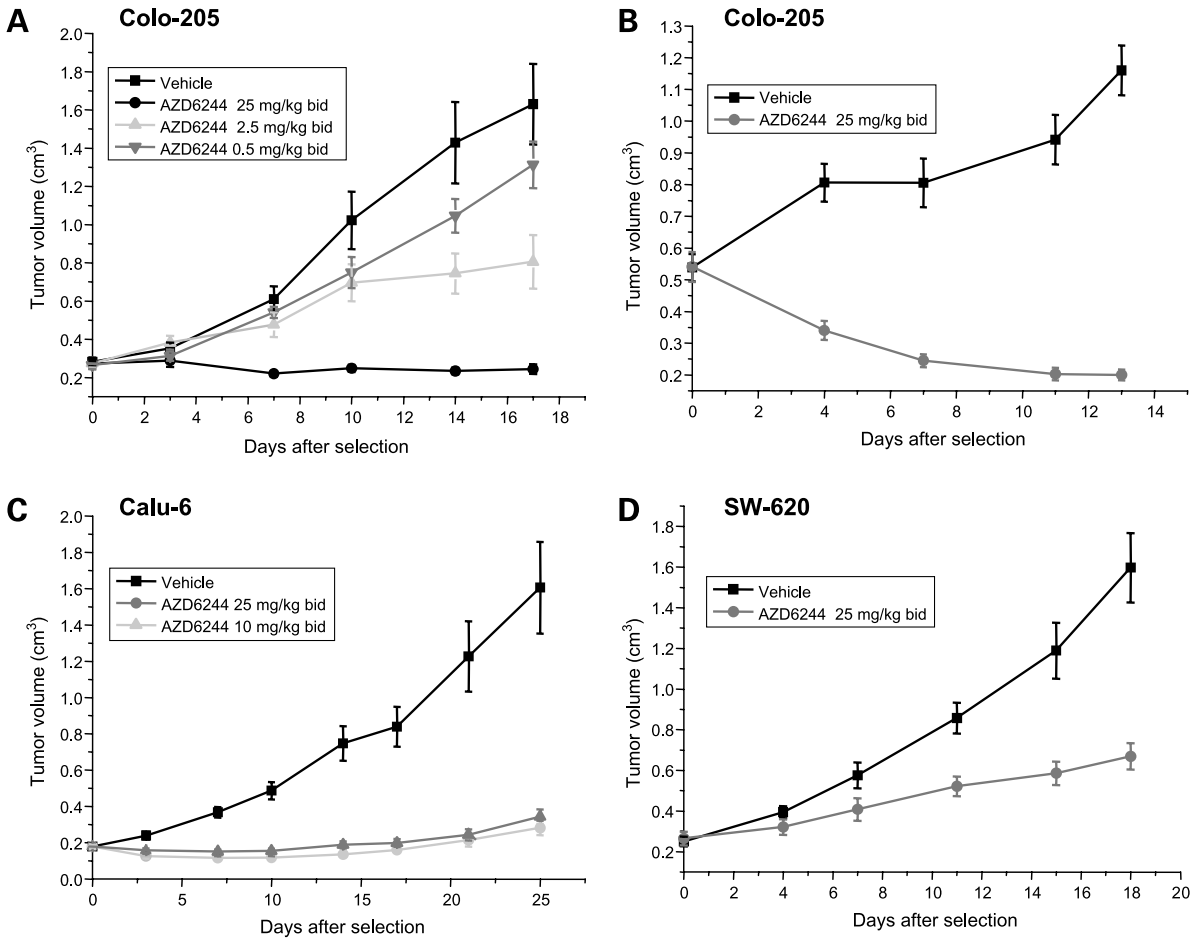

Figure 2. Effect of chronic dosing of AZD6244 on xenograft growth. **A**, Colo-205 selected at ~0.3 cm^3. **B**, Colo-205 selected at ~0.55 cm^3. **C**, Calu-6 selected at ~0.2 cm^3. **D**, SW-620 selected at ~0.2 cm^3.

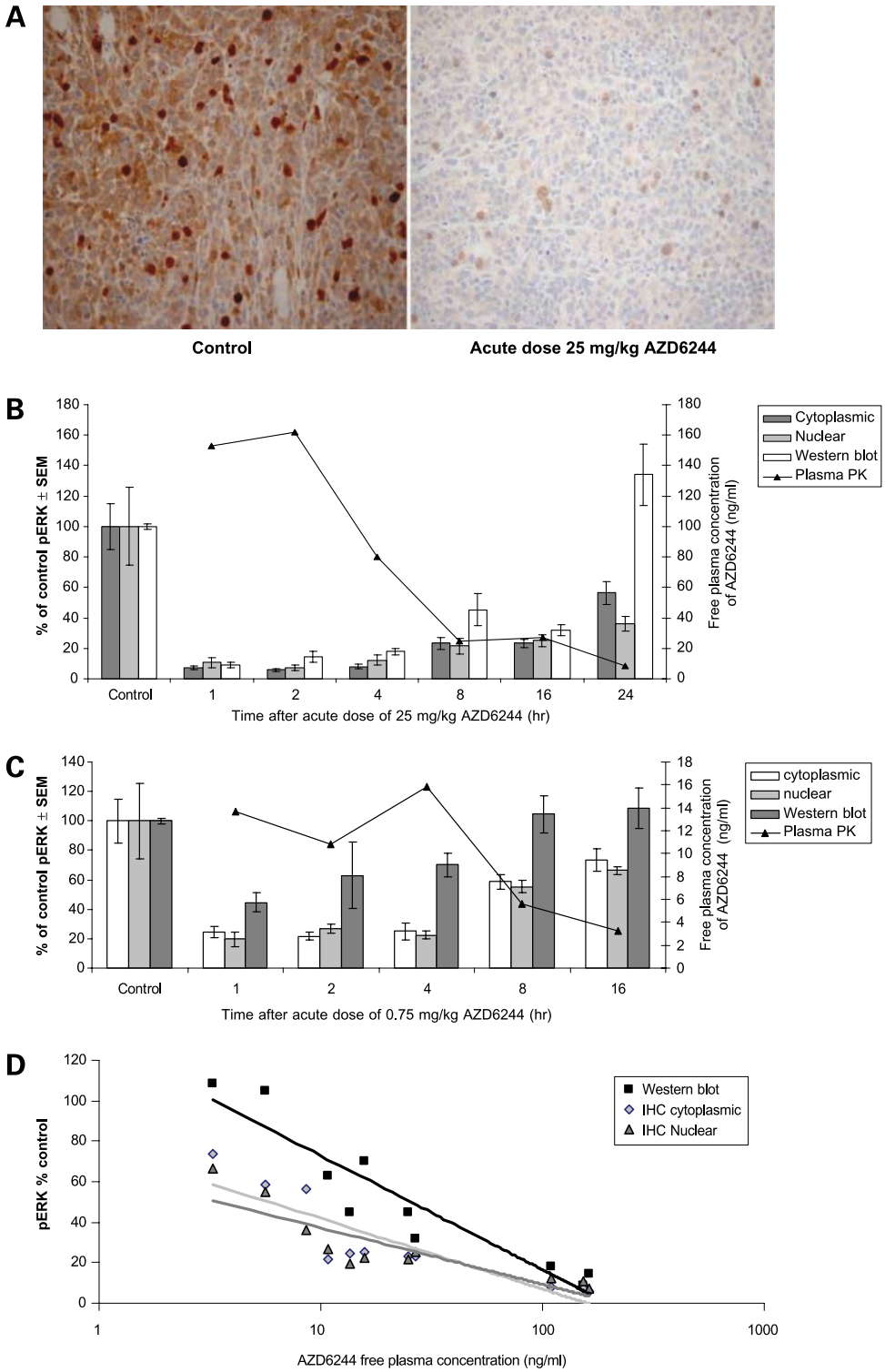

Figure 3. Pharmacodynamic effect of AZD6244 on p-ERK in Calu-6 xenografts and relationship with plasma pharmacokinetics. **A,** immunostaining for p-ERK in a control Calu-6 xenograft and in a Calu-6 xenograft 4 h after an acute dose of 25 mg/kg AZD6244. **B** and **C,** effect of an acute dose of 25 or 0.75 mg/kg AZD6244 on p-ERK in Calu-6 xenografts and free plasma concentration of drug. *PK,* pharmacokinetic. **D,** relationship between p-ERK, determined by immunocytochemistry in cytoplasm or nucleus or by Western blotting in tumor extracts, and AZD6244 plasma-free drug concentration. *IHC,* immunohistochemistry.

time point, the nuclear signal was lower than the cytoplasmic signal. The cytoplasmic signal recovered to a level that did not differ significantly from the controls after 24 h (Fig. 5A).

An acute dose of 25 mg/kg AZD6244 did not induce cleaved caspase-3 activity in this model (Fig. 5B), but BrdUrd incorporation was significantly reduced after 24 h (Fig. 5B and C).

Chronic dosing with AZD6244 seemed to induce a morphologically more differentiated phenotype in SW-620 xenografts, with small nests and glandular-like structures with clear nuclear basal polarity, whereas untreated tumors consisted of ill-defined sheets of pleiomorphic cells (Fig. 5D).

Combination of AZD6244 and Cytotoxic Drugs in SW-620 Xenografts

The SW-620 model is sensitive to the cytotoxic drugs docetaxel and irinotecan. The potential of these drugs to enhance the efficacy of AZD6244 in combination at tolerated doses was evaluated. Doses of 15 mg/kg docetaxel or 25 mg/kg irinotecan in combination with 25 mg/kg bd AZD6244 resulted in significantly enhanced efficacy than either drug alone (Fig. 6). A statistically significant interaction occurs between docetaxel and AZD6244 at these doses ($P = 0.02$), indicating a synergistic effect, whereas no significant interaction occurs between irinotecan and AZD6244 at these doses, indicating an additive effect ($P = 0.68$).

Discussion

The majority of cell lines that are sensitive (IC_{50}, <1 μmol/L) to AZD6244 *in vitro* possess a mutation in either *KRAS*, *NRAS*, or *BRAF* genes. Two other *BRAF* mutant cell lines, A2058 and MDA-MB-231, are moderately sensitive (IC_{50}, 1–10 μmol/L), but none of the resistant (>10 μmol/L) cell lines possessed a *BRAF* gene mutation. MDA-MB-231 cells carry one of the less common *BRAF* gene mutations (G464V). Although the majority of the cell lines with *KRAS* gene mutations were also sensitive, there were also some cell lines with *KRAS* gene mutations that were resistant to AZD6244 *in vitro*. These data confirm that most BRAF mutant cell lines seem to be exquisitely dependent on MEK activity and sensitive to MEK inhibition, whereas the presence of KRAS gene mutations do not seem to be as predictive of sensitivity to MEK inhibition, at least *in vitro*. The BRAF mutant cell lines SKMEL1, SKMEL3, SKMEL19, SKMEL28, MALM3M, Colo-205, and DU4475 have also been reported to be very sensitive to the MEK inhibitor CI-1040 *in vitro*, with p-ERK IC_{50}s ranging from 24 to 111 nmol/L,

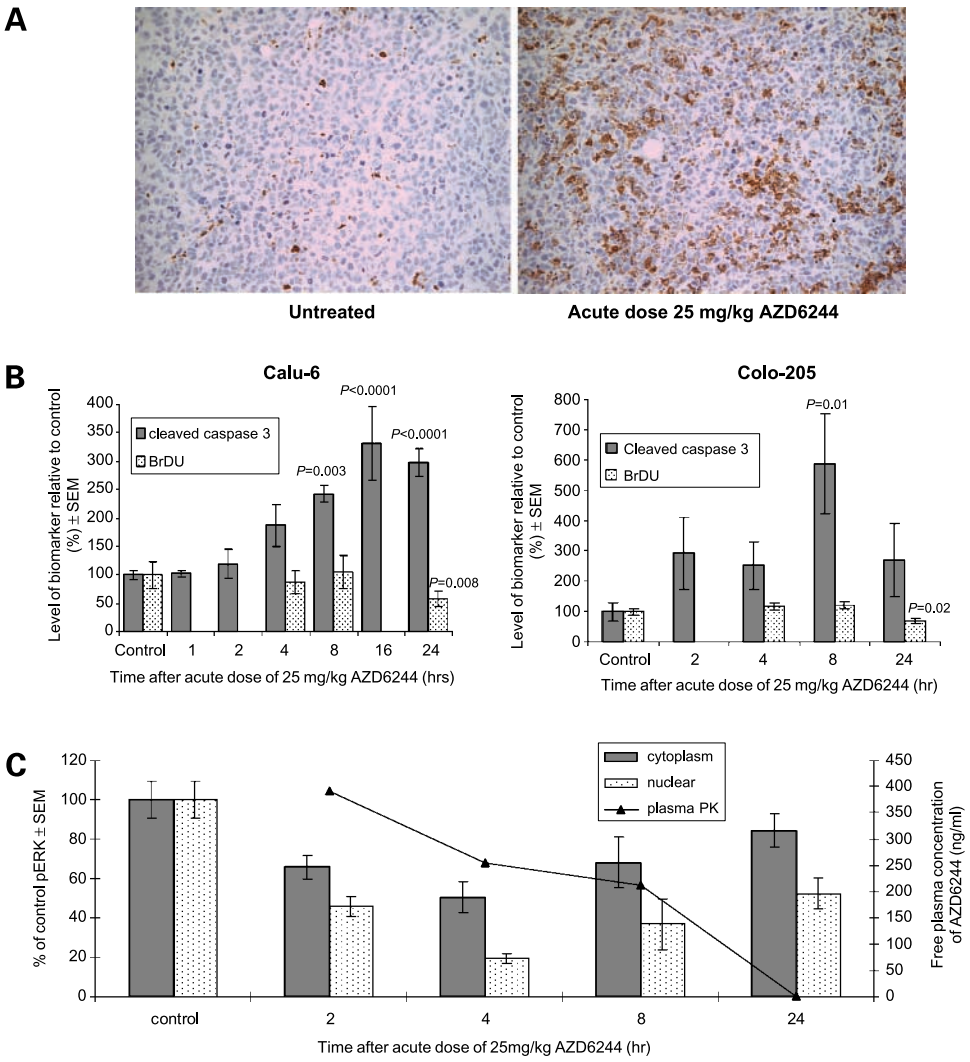

Figure 4. Pharmacodynamic effect of AZD6244 on cleaved caspase-3 and BrdUrd in Calu-6 and Colo-205 xenografts. **A**, immunostaining for cleaved caspase-3 in an untreated control Calu-6 xenograft and a Calu-6 xenograft 24 h after an acute dose of 25 mg/kg AZD6244. **B**, image analysis of immunohistochemical staining for cleaved caspase-3 and BrdUrd in Calu-6 and Colo-205 and xenografts after a single acute dose of 25 mg/kg AZD6244. **C**, relationship between inhibition of p-ERK in Colo-205 xenografts and free plasma concentration of drug following an acute dose of 25 mg/kg AZD6244.

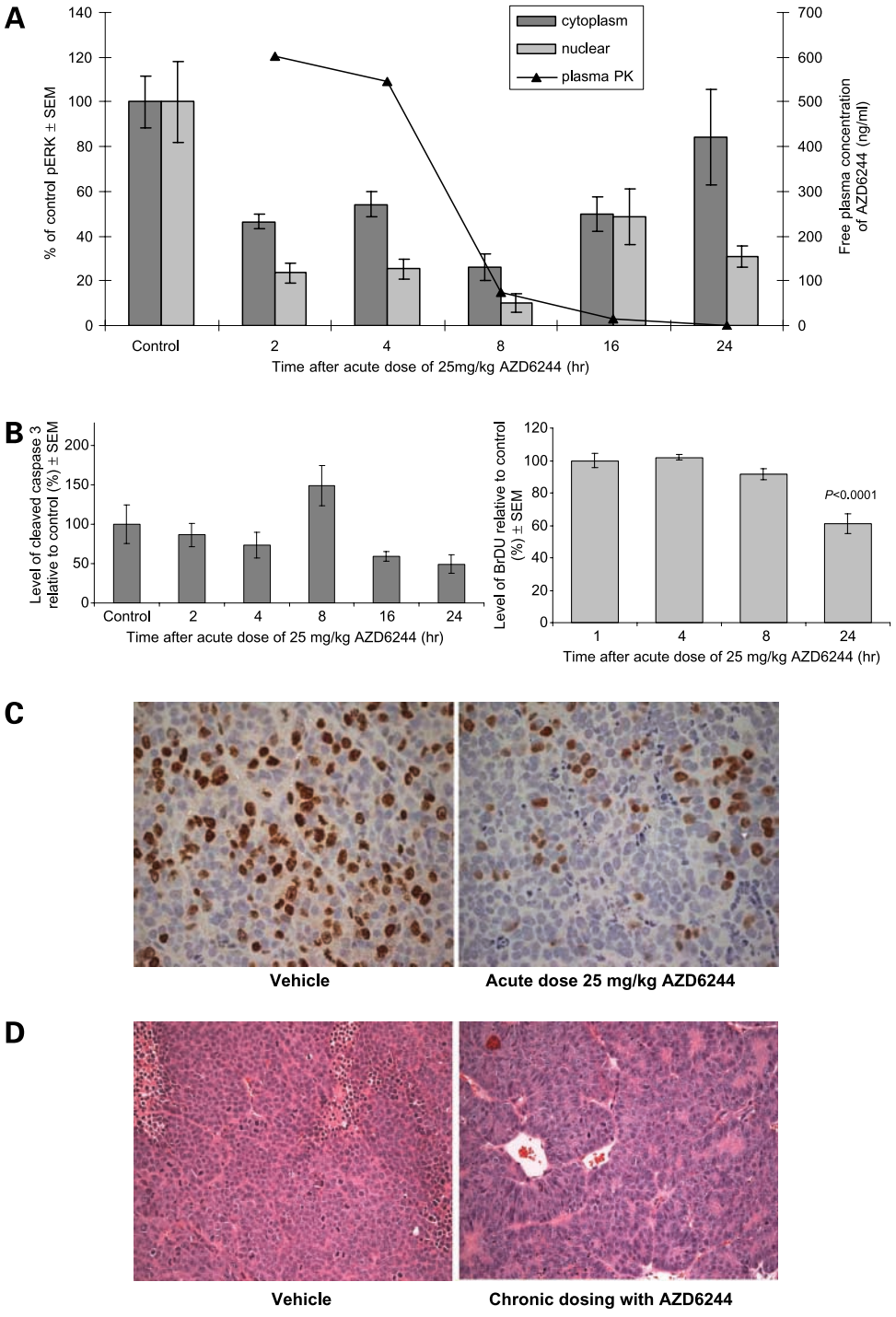

Figure 5. Pharmacodynamic effects of AZD6244 on SW-620 xenografts. **A,** relationship between inhibition of p-ERK in SW-620 xenografts and free plasma concentration of drug following an acute dose of 25 mg/kg AZD6244. **B,** image analysis of immunohistochemical staining for cleaved caspase-3 and BrdUrd in SW-620 xenografts after an acute dose of 25 mg/kg AZD6244. **C,** immunostaining for BrdUrd in an untreated control SW-620 xenograft and a SW-620 xenograft 24 h after an acute dose of 25 mg/kg AZD6244. **D,** H&E staining showing morphology of SW-620 xenografts in untreated mice and mice chronically dosed with AZD6244.

and another specific MEK inhibitor, PD0325901, completely suppressed the growth of SKMEL28 and Colo-205 xenografts *in vivo* when dosed at 5 mg/kg/d (15). Our finding that KRAS mutant cell lines can be both sensitive and insensitive *in vitro* to AZD6244 extends the observations made by Solit et al. (15) using CI-1040 and suggests that both BRAF and RAS gene mutation can confer high sensitivity to MEK inhibition. The greater variability in sensitivity among the KRAS mutant cell lines may be explained by the greater promiscuity of *ras* proteins, which initiate signaling through several other major signaling pathways that have been implicated in cancer development, such as the phosphatidylinositol 3-kinase pathway, whereas MEK1/2 kinases are the only widely recognized substrates of *raf* proteins.

The efficacy of AZD6244 was evaluated in nude mice bearing xenografts from cells with B-raf or K-ras mutations that are highly sensitive (Colo-205, Calu-6, and SW-620) to AZD6244 *in vitro*. Chronic twice-daily dosing of 25 mg/kg AZD6244 caused stasis of Colo-205 tumors if dosing was commenced when the tumors were small (~0.2 cm^3) and partial regression if dosing was commenced when the tumors were larger (~0.55 cm^3). The same dosing schedule of AZD6244 inhibited Calu-6 tumor growth strongly (94% inhibition) and SW-620 tumor growth moderately (73% inhibition). These experiments confirmed that *in vitro* sensitivity broadly predicts *in vivo* efficacy in the cell lines selected. It should be noted that AZD6244 *in vivo* efficacy has also been shown in xenografts that have both K-ras and B-raf wild-type genes, such as BxPC3 (13).

Inhibition of ERK phosphorylation, the unique substrate of MEK and primary biomarker for AZD6244, and its relationship with plasma concentration of AZD6244 was evaluated in this panel of sensitive xenografts. Calu-6 showed a higher constitutive expression of p-ERK than SW-620 and Colo-205 xenografts. The percentage inhibition was greater and the time required to maximally inhibit p-ERK was shorter in Calu-6 than in Colo-205 and SW-620 xenografts. In mice bearing Calu-6 xenografts, an acute dose of 25 mg/kg AZD6244 was sufficient to inhibit p-ERK by >90% after 1 h and maintain p-ERK inhibition by >50% for at least 16 h regardless of whether p-ERK levels were determined by immunocytochemistry or Western blotting. After an acute dose of 0.75 mg/kg, the percentage reduction in p-ERK levels detected by immunocytochemistry was consistently lower than by Western blotting, but the data showed a similar trend. When inhibition of ERK phosphorylation was plotted against free plasma concentration of AZD6244, the IC_{50}s extrapolated from the immunocytochemistry signals correlated more closely with the IC_{50} for p-ERK inhibition determined *in vitro* in Calu-6 cells (4.4 nmol/L or 2 ng/mL). Inhibition of p-ERK, measured by immunocytochemistry, recovered to slightly >50% of control by 8 h following an acute dose of 0.75 mg/kg AZD6244 (the minimum twice-daily dose required for antitumor activity). Hence, twice daily dosing to achieve >50% p-ERK inhibition for ~16 h seems to be required for significant antitumor activity in the Calu-6 model.

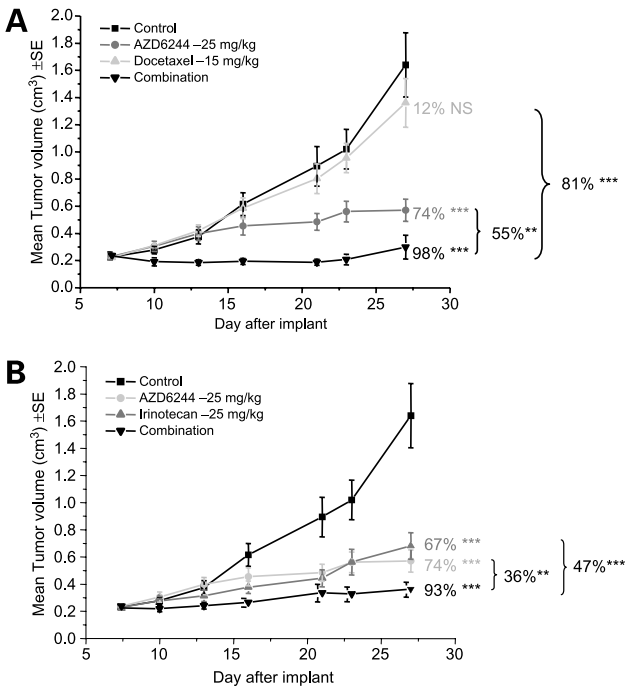

Figure 6. The effect of combination of AZD6244 with docetaxel or irinotecan on the growth of SW-620 xenografts. SW-620 selected at ~0.2 cm^3. **A**, effect of AZD6244 in combination with docetaxel or each compound alone after 21 d of treatment. **B**, effect of AZD6244 in combination with irinotecan or each compound alone after 21 d of treatment.

The percentage inhibition of ERK phosphorylation detected by immunocytochemistry in Colo-205 and SW-620 xenografts after an acute dose of 25 mg/kg AZD6244 was significant but of lesser magnitude than detected after the same dose in Calu-6 xenografts. In these models, the percentage inhibition of the cytoplasmic signal was consistently less than the nuclear signal, and the maximum reduction in p-ERK levels lagged behind the peak plasma concentration. The reason for the reduced magnitude of p-ERK inhibition detected in the Colo-205 and SW-620 tumors is unclear, but it may be explained, at least in part, by a limitation of the image analysis method. The relatively low level of constitutive p-ERK expression in Colo-205 and SW-620 tumors compared with Calu-6 tumors results in a higher signal-to-noise ratio and, consequently, a lower dynamic range of the p-ERK signal in these tumors.

In the two most sensitive xenografts, a single dose of AZD6244 was sufficient to induce apoptosis. In the Colo-205 model, which is most sensitive to AZD6244 *in vitro*, the fold induction of the apoptotic marker cleaved caspase-3 *in vivo* was greater than that seen in Calu-6 xenografts. In the moderately sensitive SW-620 model, no induction of apoptosis was observed. Rather, these tumors responded to a single dose of AZD6244 by a reduction in cell proliferation, as indicated by a reduced S-phase fraction, and, after chronic dosing, induction of a more differentiated phenotype. A significant reduction in BrdUrd incorporation was also seen after 24 h in Calu-6 and Colo-205 xenografts, but because these tumors contain large areas of apoptotic and dead cells following treatment, the reduction in BrdUrd signal may not represent a reduction in the S-phase fraction of the remaining viable tumor cell population.

Induction of the apoptotic marker cleaved caspase-3 occurs more rapidly than reduction in BrdUrd incorporation, suggesting that changes in transcriptional activity are probably necessary to mediate the reduction in S-phase fraction in SW-620 cells, whereas the apoptotic phenotype is more likely to be a direct consequence of

inhibiting cell signaling downstream of MEK. The reduction in cell proliferation is most likely ultimately due to modulation of transcription of genes that encode cell cycle proteins by transcription factors that are phosphorylated by ERK. For example, ERK can phosphorylate Elk1 (16, 17), which then regulates the transcription of c-fos. Moreover, when inactivation of ERK is delayed, direct phosphorylation of c-fos by ERK stabilizes fos protein (18). *fos* is one of several important ''early genes'' required for transcription of essential cell cycle proteins required for the G_1-S transition. G_1 cell cycle arrest in cells following MEK inhibition has been found to correlate with down-regulation of cyclin D1 protein expression, loss of RB phosphorylation, and increases in p27 cyclin-dependent kinase inhibitor (15). Other mechanisms may also account for reduced cell proliferation; for example, inhibition of MEK could also inhibit ERK-dependent phosphorylation of the tumor suppressor TSC2 and therefore enhance its ability to inhibit mammalian target of rapamycin signaling (19), resulting in reduced cell proliferation. Chronic suppression of cell proliferation as a result of sustained MEK inhibition leads to expression of more differentiated phenotypes in the SW-620 xenografts; this is not seen after an acute dose. We have also observed altered morphology in the HT-29 colorectal cancer xenograft model following chronic dosing with AZD6244; in this model, the xenografts had less necrosis, a higher proportion of goblet-like cells, and more intervening fibrous stroma when compared with control xenografts (data not shown).

There are various mechanisms by which MEK inhibitors may enhance apoptosis and these may vary between cell types. ERK can inhibit the activity of various proapoptotic proteins by direct phosphorylation, including caspase-9 (20), Bim-EL (21), IEX1 (22), and Bad (23–25). Activated ERKs can also phosphorylate and enhance the activity of the Bcl2 family members Bcl-2 and Mcl-1, and recently, MEK inhibition has been shown to cause a reduction in Mcl-1 levels in acute myelogenous leukemia cells (26–28). CI-1040 induced apoptosis in acute lymphocytic leukemia cells *in vitro* through a pathway involving dephosphorylation and aggregation of Fas-associated death domain protein followed by caspase-8 activation (29).

The reason why some xenografts respond to AZD6244 by inhibition of cell proliferation, whereas others are sensitized to apoptosis, is unclear. It may reflect differences in ERK substrate expression or differential cell signaling networks in tumor cells, which may be a consequence of mutations in genes encoding proteins that modulate the signals downstream of MEK. It is also very possible that the cellular response to MEK signaling is modulated by the tumor microenvironment *in vivo*, such as the extent of hypoxia, growth factor availability, and stroma-tumor interactions. This may, in part, explain why SW-620 cells are less responsive to AZD6244 *in vivo* than Calu-6 cells, whereas the opposite is true *in vitro*. Although it is possible to speculate for instance that p53 might modulate responses, it will be necessary to study a larger number of model systems to allow any firm conclusions to be drawn about molecular determinants of the AZD6244 response. The construction of tissue microarrays will help us to understand better which, if any, of these mechanisms underlie the *in vivo* effects of MEK inhibition, and this may provide an insight into new therapeutic targets and identify more predictive biomarkers of response.

The combination of AZD6244 with either docetaxel or irinotecan results in significantly greater antitumor activity than the same dose of either agent alone. This effect was particularly striking with AZD6244 and docetaxel, where a significant interaction was seen between the two compounds, indicating synergy. The combination of other MEK inhibitors (U0126 or PD98059) and paclitaxel has been shown to dramatically enhance apoptosis by up to four times more than the additive value of the two drugs alone in H157 human lung and OVCA194 ovarian carcinoma cells *in vitro* (30). Paclitaxel activates the MEK/ERK pathway and compromises its own activity, which activates apoptosis via the c-Jun NH_2-terminal kinase pathway. Enhancement of the therapeutic efficacy of Taxol by CI-1040 has also been shown in nude mice bearing human non–small cell lung cancer heterotransplants (31). CI-1040 alone increased the expression of S473-phosphorylated Akt in several of these heterotransplants, whereas the concurrent combination of CI-1040 and Taxol resulted in lower S473-phosphorylated Akt, suggesting that inhibition of MEK can reciprocally activate Akt. Similar findings have been reported with U0126 and Taxol *in vitro* (32). However, tumors from mice treated with both agents also showed down-regulation of proliferating cell nuclear antigen and vascular endothelial growth factor expression relative to single-agent treatment, which may also contribute to the enhanced efficacy of the combination. Moreover, the accumulation of cells in the G_2-M phase of the cell cycle after treatment with taxanes, leading to increased abundance of MEK, may also explain the enhanced efficacy of the combination of taxanes and MEK inhibitors.

In summary, p-ERK has been validated as a robust biomarker of AZD6244 activity in human tumor xenografts growing in nude mice using both immunohistochemistry and Western blotting of *ex vivo* tumor tissue. In Calu-6 xenografts, we observed a comparable trend in the data using immunocytochemistry and Western blotting, and the cytoplasmic signal by immunocytochemistry most closely correlated with the IC_{50} *in vitro* for inhibition of ERK phosphorylation in cultured cells. AZD6244 has a proapoptotic mechanism of action in the two xenograft models most sensitive to AZD6244 (i.e., Colo-205 and Calu-6), whereas it induces differentiation and has an antiproliferative mechanism of action in the less sensitive SW-620 model. Therefore, AZD6244 treatment can be antiproliferative and proapoptotic and able to induce differentiation depending on the tumor type. Moreover, AZD6244 has potential as a combination therapy with the cytotoxic drugs irinotecan and docetaxel.

References

1. Adjei AA. Blocking oncogenic Ras signaling for cancer therapy. J Natl Cancer Inst 2001;93:1062 – 74.

2. Sieben NL, Macropoulos P, Roemen GM, et al. In ovarian neoplasms, BRAF, but not KRAS, mutations are restricted to low-grade serous tumours. J Pathol 2004;202:336 – 40.

3. Aviel-Ronen S, Blackhall FH, Shepherd FA, Tsao MS. K-ras mutations in non-small-cell lung carcinoma: a review. Clin Lung Cancer 2006;8: 30 – 8.

4. Davies H, Bignell GR, Cox C, et al. Mutations of the BRAF gene in human cancer. Nature 2002;417:949 – 54.

5. Thomas NE. BRAF somatic mutations in malignant melanoma and melanocytic naevi. Melanoma Res 2006;16:97 – 103.

6. Cohen Y, Xing M, Mambo E, et al. BRAF mutation in papillary thyroid carcinoma. J Natl Cancer Inst 2003;95:625 – 7.

7. Kimura ET, Nikiforova MN, Zhu Z, Knauf JA, Nikiforov YE, Fagin JA. High prevalence of BRAF mutations in thyroid cancer: genetic evidence for constitutive activation of the RET/PTC-RAS-BRAF signaling pathway in papillary thyroid carcinoma. Cancer Res 2003;63:1454 – 7.

8. Singer G, Oldt R III, Cohen Y, et al. Mutations in BRAF and KRAS characterize the development of low-grade ovarian serous carcinoma. J Natl Cancer Inst 2003;95:484 – 6.

9. Yuen ST, Davies H, Chan TL, et al. Similarity of the phenotypic patterns associated with BRAF and KRAS mutations in colorectal neoplasia. Cancer Res 2002;62:6451 – 5.

10. Brose MS, Volpe P, Feldman M, et al. BRAF and RAS mutations in human lung cancer and melanoma. Cancer Res 2002;62:6997 – 7000.

11. Yoon S, Seger R. The extracellular signal-regulated kinase: multiple substrates regulate diverse cellular functions. Growth Factors 2006;24: 21 – 44.

12. Hanahan D, Weinberg RA. The hallmarks of cancer. Cell 2000;100: 57 – 70.

13. Yeh TC, Marsh V, Bernat BA, et al. Biological characterisation of ARRY-142886 (AZD6244), a potent, highly selective mitogen-activated protein kinase kinase 1/2 inhibitor. Clin Cancer Res 2007;13:1576 – 83.

14. Chow LQM, Eckhardt SG, Reid J, et al. A first in human dose-ranging study to assess the pharmacokinetics, pharmacodynamics, and toxicities of the MEK inhibitor, ARRY-142886 (AZD6244), in patients with advanced solid malignancies [abstract C162]. Clin Cancer Res 2006;11.

15. Solit DB, Garraway LA, Pratilas CA, et al. BRAF mutation predicts sensitivity to MEK inhibition. Nature 2006;439:358 – 62.

16. Gille H, Sharrocks AD, Shaw PE. Phosphorylation of transcription factor p62TCF by MAP kinase stimulates ternary complex formation at c-fos promoter. Nature 1992;358:414 – 7.

17. Cruzalegui FH, Cano E, Treisman R. ERK activation induces phosphorylation of Elk-1 at multiple S/T-P motifs to high stoichiometry. Oncogene 1999;18:7948 – 57.

18. Murphy LO, Smith S, Chen RH, Fingar DC, Blenis J. Molecular interpretation of ERK signal duration by immediate early gene products. Nat Cell Biol 2002;4:556 – 64.

19. Ma L, Chen Z, Erdjument-Bromage H, Tempst P, Pandolfi PP. Phosphorylation and functional inactivation of TSC2 by Erk implications for tuberous sclerosis and cancer pathogenesis. Cell 2005;121:179 – 93.

20. Allan LA, Morrice N, Brady S, Magee G, Pathak S, Clarke PR. Inhibition of caspase-9 through phosphorylation at Thr 125 by ERK MAPK. Nat Cell Biol 2003;5:647 – 54.

21. Biswas SC, Greene LA. Nerve growth factor (NGF) down-regulates the Bcl-2 homology 3 (BH3) domain-only protein Bim and suppresses its proapoptotic activity by phosphorylation. J Biol Chem 2002;277: 49511 – 6.

22. Garcia J, Ye Y, Arranz V, Letourneux C, Pezeron G, Porteu F. IEX-1: a new ERK substrate involved in both ERK survival activity and ERK activation. EMBO J 2002;21:5151 – 63.

23. Scheid MP, Schubert KM, Duronio V. Regulation of bad phosphorylation and association with Bcl-x(L) by the MAPK/Erk kinase. J Biol Chem 1999;274:31108 – 13.

24. She QB, Solit DB, Ye Q, O'Reilly KE, Lobo J, Rosen N. The BAD protein integrates survival signaling by EGFR/MAPK and PI3K/Akt kinase pathways in PTEN-deficient tumor cells. Cancer Cell 2005;8:287 – 97.

25. Eisenmann KM, VanBrocklin MW, Staffend NA, Kitchen SM, Koo HM. Mitogen-activated protein kinase pathway-dependent tumor-specific survival signaling in melanoma cells through inactivation of the proapoptotic protein bad. Cancer Res 2003;63:8330 – 7.

26. Deng X, Ruvolo P, Carr B, May WS, Jr. Survival function of ERK1/2 as IL-3-activated, staurosporine-resistant Bcl2 kinases. Proc Natl Acad Sci USA 2000;97:1578 – 83.

27. Domina AM, Vrana JA, Gregory MA, Hann SR, Craig RW. MCL1 is phosphorylated in the PEST region and stabilized upon ERK activation in viable cells, and at additional sites with cytotoxic okadaic acid or taxol. Oncogene 2004;23:5301 – 15.

28. Konopleva M, Contractor R, Tsao T, et al. Mechanisms of apoptosis sensitivity and resistance to the BH3 mimetic ABT-737 in acute myeloid leukemia. Cancer Cell 2006;10:375 – 88.

29. Meng XW, Chandra J, Loegering D, et al. Central role of Fas-associated death domain protein in apoptosis induction by the mitogen-activated protein kinase kinase inhibitor CI-1040 (PD184352) in acute lymphocytic leukemia cells *in vitro*. J Biol Chem 2003;278:47326 – 39.

30. MacKeigan JP, Collins TS, Ting JP. MEK inhibition enhances paclitaxel-induced tumor apoptosis. J Biol Chem 2000;275:38953 – 6.

31. McDaid HM, Lopez-Barcons L, Grossman A, et al. Enhancement of the therapeutic efficacy of taxol by the mitogen-activated protein kinase kinase inhibitor CI-1040 in nude mice bearing human heterotransplants. Cancer Res 2005;65:2854 – 60.

32. MacKeigan JP, Taxman DJ, Hunter D, Earp HS III, Graves LM, Ting JP. Inactivation of the antiapoptotic phosphatidylinositol 3-kinase-Akt pathway by the combined treatment of taxol and mitogen-activated protein kinase kinase inhibition. Clin Cancer Res 2002;8:2091 – 9.

Molecular Cancer Therapeutics

AZD6244 (ARRY-142886), a potent inhibitor of mitogen-activated protein kinase/extracellular signal-regulated kinase kinase 1/2 kinases: mechanism of action *in vivo*, pharmacokinetic/pharmacodynamic relationship, and potential for combination in preclinical models

Barry R. Davies, Armelle Logie, Jennifer S. McKay, et al.

Mol Cancer Ther 2007;6:2209-2219.